ELSEVIER

Cardiovascular Research 76 (2007) 409–417

Cardiovascular Research

www.elsevier.com/locate/cardiores

A novel C-terminal truncation *SCN5A* mutation from a patient with sick sinus syndrome, conduction disorder and ventricular tachycardia

Bi-Hua Tan [a,1], Pedro Iturralde-Torres [b,1], Argelia Medeiros-Domingo [c,d,e,f], Santiago Nava [b], David J. Tester [d,e,f], Carmen R. Valdivia [a], Teresa Tusié-Luna [c], Michael J. Ackerman [d,e,f], Jonathan C. Makielski [a,*]

[a] *Department of Medicine, Cardiovascular Section, University of Wisconsin-Madison, 600 Highland Ave H6/349, Madison, WI 53792, United States*
[b] *Instituto Nacional de Cardiología "Ignacio Chávez", Mexico*
[c] *Instituto de Investigaciones Biomédicas, UNAM, Instituto Nacional de Ciencias Médicas y Nutrición, SZ, Mexico*
[d] *Department of Medicine, Division of Cardiovascular Diseases, Mayo Clinic College of Medicine, Rochester, MN, United States*
[e] *Department of Pediatrics, Division of Pediatric Cardiology, Mayo Clinic College of Medicine, Rochester, MN, United States*
[f] *Department of Molecular Pharmacology and Experimental Therapeutics, Mayo Clinic College of Medicine, Rochester, MN, United States*

Received 22 March 2007; received in revised form 24 July 2007; accepted 15 August 2007
Available online 22 August 2007
Time for primary review 22 days

Abstract

Objectives: Individual mutations in the *SCN5A*-encoding cardiac sodium channel α-subunit cause single cardiac arrhythmia disorders, but a few cause multiple distinct disorders. Here we report a family harboring an *SCN5A* mutation (L1821fs/10) causing a truncation of the C-terminus with a marked and complex biophysical phenotype and a corresponding variable and complex clinical phenotype with variable penetrance.
Methods and results: A 12-year-old male with congenital sick sinus syndrome (SSS), cardiac conduction disorder (CCD), and recurrent monomorphic ventricular tachycardia (VT) had mutational analysis that identified a 4 base pair deletion (TCTG) at position 5464–5467 in exon 28 of *SCN5A*. The mutation was also present in six asymptomatic family members only two of which showed mild ECG phenotypes. The deletion caused a frame-shift mutation (L1821fs/10) with truncation of the C-terminus after 10 missense amino acid substitutions. When expressed in HEK-293 cells for patch-clamp study, the current density of L1821fs/10 was reduced by 90% compared with WT. In addition, gating kinetic analysis showed a 5-mV positive shift in activation, a 12-mV negative shift of inactivation and enhanced intermediate inactivation, all of which would tend to reduce peak and early sodium current. Late sodium current, however, was increased in the mutated channels.
Conclusions: The L1821fs/10 mutation causes the most severe disruption of SCN5A structure for a naturally occurring mutation that still produces current. It has a marked loss-of-function and unique phenotype of SSS, CCD and VT with incomplete penetrance.

Keywords: Genetics; Arrhythmia; Sick sinus syndrome; Conduction disorder; Ventricular tachycardia; *SCN5A*; Sodium current; Frame-shift mutation, $Na_v1.5$; Inherited arrhythmia

This article is referred to in the Editorial by van Rijen and de Bakker (pages 379–380) in this issue.

1. Introduction

SCN5A encodes the voltage-dependent sodium channel α-subunit protein $hNa_v1.5$ [1], found predominantly in human heart muscle. This channel is responsible for large peak inward sodium current (I_{Na}) that underlies excitability and conduction in working myocardium (atrial and ventricular cells) and special conduction tissue (Purkinje cells and others), and also for late I_{Na} that influences repolarization and refractoriness.

* Corresponding author. Tel.: +1 608 263 9648; fax: +1 608 263 0405.
E-mail address: jcm@medicine.wisc.edu (J.C. Makielski).
[1] Contributed equally to this study.

0008-6363/$ - see front matter © 2007 European Society of Cardiology. Published by Elsevier B.V. All rights reserved.
doi:10.1016/j.cardiores.2007.08.006

Mutations in *SCN5A* that increase late I_{Na} ("gain of function") cause type 3 long QT syndrome (LQT3) [2], and mutations that decrease peak I_{Na} ("loss of function") cause several arrhythmogenic syndromes including type 1 Brugada syndrome (BrS1) [3] and isolated cardiac conduction disease (ICCD) [4,5]. More rarely, congenital sick sinus syndrome (SSS) has also been linked to mutations in *SCN5A* [6,7].

To date, at least 4 mutations in the cardiac sodium channel have been identified whereby the same mutation precipitated multiple different disease phenotypes [7–10]. An insertion of an aspartic acid residue in the C-terminus of *SCN5A* (1795insD) can result in either BrS1 or LQT3 [8]. The mutation of glycine to arginine (G1406R in the original publication, G1408R by present numbering) in the DIII/S5 to DIII/S6 region resulted in either BrS1 or ICCD in several families [9]. The deletion of a lysine in the III–IV linker of SCN5A (ΔK1500) is associated with BrS1, LQT3 and ICCD [10]. A replacement of glutamic acid by the basic residue lysine (E161K) in the DI/S2 transmembrane region contributes to SSS, CCD and BrS1 [7]. The mechanisms by which the same or similar biophysical phenotype such as loss-of-function can cause multiple distinct clinical phenotypes are unknown. Discovering and characterizing additional novel mutations in families showing multiple phenotypes may provide further insight.

The sodium channel C-terminal domain (residues 1773–2016) represents a crucial structure implicated in channel inactivation modulation [11]. Intramolecular interactions between $Na_v1.5$ III–IV linker and C-terminal domain have been implicated in stabilization of the inactivated state. Estimated three-dimensional structure predicts that the proximal half contains six helical structures, while the distal half consists of an unstructured peptide. Functional experiments revealed no role of the distal unstructured C-terminal domain. Truncation of the predicted sixth helix of the structured C-terminal region uncouples the C-terminal from the III–IV linker [11]. To date, no deletions in this C-terminal domain have been associated with any heritable arrhythmia syndromes. We present a unique phenotype and functional characterization of a case involving a 4 base deletion (TCTG) in *SCN5A* at position 5464–5467 in exon 28. This deletion produces a frame-shift mutation (L1821fs/10) that deletes the terminal 195 amino acids. This severe, premature truncation includes amino acids comprising the predicted sixth helix.

Despite a severe disruption of the channel structure, L1821fs/10-SCN5A produced currents, albeit reduced, with predominantly loss-of-function but also an increase in late I_{Na} relative to peak. The corresponding clinical phenotype was complex with SSS, CCD and recurrent monomorphic ventricular tachycardia (VT).

2. Methods

2.1. Mutational analysis of SCN5A

Comprehensive open reading frame/splice site mutational analysis of *SCN5A* was performed using denaturing high performance liquid chromatography (DHPLC), and direct DNA sequencing as previously described [12,13]. The study was performed according to the terms required by the Research Ethics Committee of the National Institute of Cardiology "Ignacio Chávez", México City and the Mayo Foundation Institution Review Board written informed consent was obtained from all participants. The investigation also conforms with the principles outlined in the "Declaration of Helsinki" (Cardiovascular Research 1997; 35:2–4).

2.2. Site-directed mutagenesis and heterologous expression

L1821fs/10 was created by site-direct mutagenesis (mutagenesis kit from Stratagene®) using a PCR technique. The appropriate nucleotide changes for L1821fs/10 were engineered into the most common splice variant of human cardiac voltage-dependent Na channel *SCN5A*/$hNa_v1.5$ [lacking a glutamine at position 1077, we note as Q1077del (Genbank accession No. AY148488)] in the pcDNA3 vector (Invitrogen; Carlsbad, CA). Integrity of the constructs was verified by DNA sequencing. WT and mutant channels were transiently expressed in HEK-293 cells for functional study as described previously [14,15].

2.3. Standard electrophysiological measurements for functional characterization

Macroscopic I_{Na} was measured using a standard whole-cell patch-clamp method at a temperature of 22–24 °C. Details have been previously published [15]. The extracellular (bath) solution contained, in mmol/L, NaCl 140, KCl 4, $CaCl_2$ 1.8, $MgCl_2$ 0.75 and HEPES 5 (pH 7.4 set with NaOH). The pipette solution contained, in mmol/L, CsF 120, CsCl 20, EGTA 2 and HEPES 5 (pH 7.4 set with CsOH). Pipettes had resistances between 1.0 and 2.0 MΩ when filled with recording solution. The data were acquired using pClamp 8.2 (Axon Instruments Inc.Union City, CA) and analyzed using Clampfit (Axon Instruments Inc.). The standard voltage clamp protocols are presented with the data and as described in detail previously [16].

2.4. Immunocytochemistry

Forty-eight hours post-transfection, HEK-293 cells transfected with WT and mutant plasmid DNA containing the FLAG epitope, which introduced between S1 and S2 in domain I of $hNa_v1.5$ were used for the immunocytochemistry experiments using confocal microscopy. Transfected and nontransfected HEK-293 cells were fixed with a freshly prepared mixture of methanol: acetone (1:1) for 1 min. Other details of the procedure have been previously published [17].

2.5. Statistic analysis

Data are shown as symbols with standard error of the mean (S.E.M.). Determinations of statistical significance

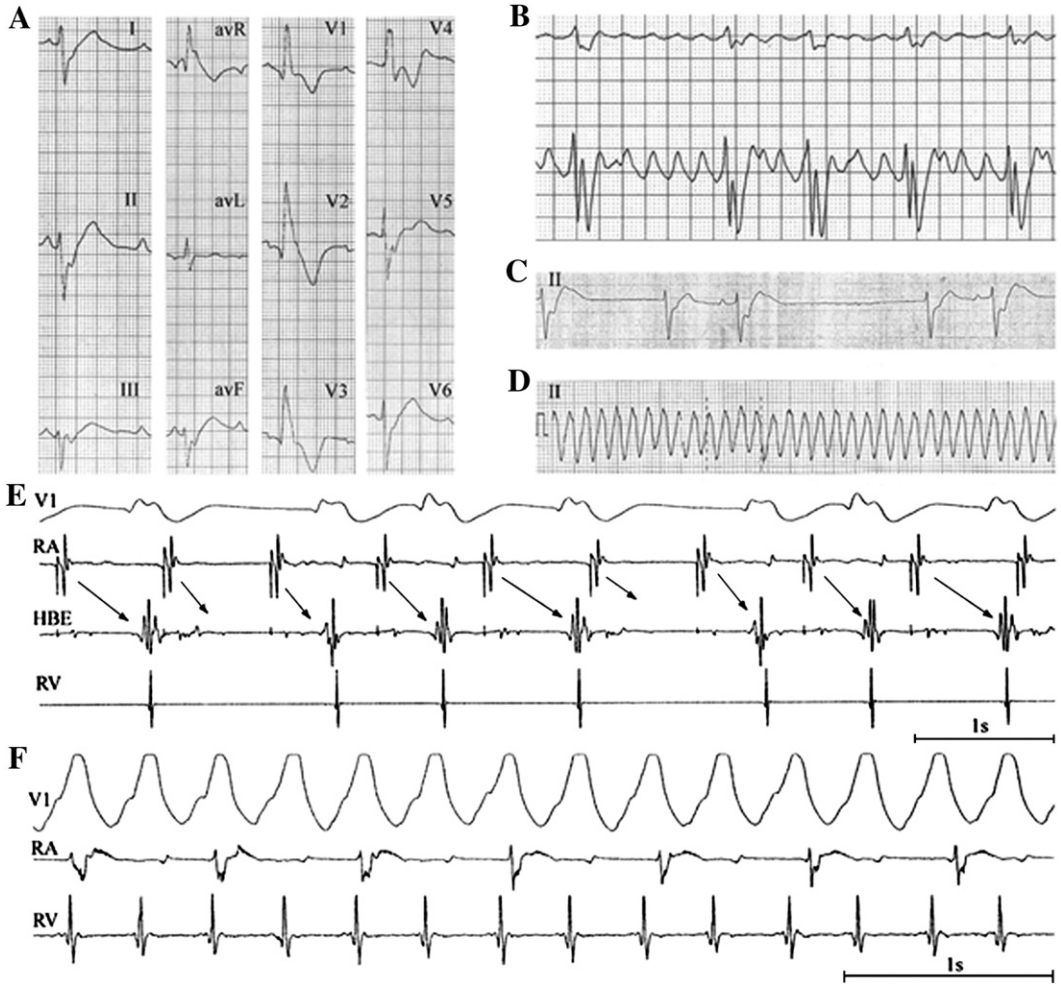

Fig. 1. Electrocardiographic phenotypes. (A) 12-lead surface ECG (10 mm/mV, 25 mm/s, 71 bpm) from proband at 1 year of age showing a prolonged QRS (160 ms) duration with a typical right bundle branch configuration and a prolonged QT interval. (B) 24-h Holter monitoring shows atrial flutter with 3:1 to 6:1 atrioventricular (AV) conduction. (C) Lead II ECG (10 mm/mV, 25 mm/s) shows sinus bradycardia and sinus pause up to 3.72 s and junctional escapes. (D) Lead II ECG (5 mm/mV, 12.5 mm/s) shows monomorphic ventricular tachycardia with a heart rate of 200 bpm. (E) Intracardiac ECG (V1—surface V1 lead, RA and RV—right atrium and ventricular, HBE—His bundle electrogram) shows a second-degree AV block with 4:3 AV conduction during AAI pacing at 80 bpm. (F) Intracardiac ECG shows an induced monomorphic VT (heart rate 171 bpm) and AV dissociation.

were performed using one-way ANOVA for comparisons of two groups. A p value of <0.05 was considered statistically significant. Curve fits are down using pClamp 8.2 (Axon Instruments). Non-linear curve fitting is performed with Origin 6.0 (Microcal Software).

3. Results

3.1. Clinical case

A 12-year-old male presented with fetal bradycardia and no family history of cardiac disease or sudden death. He was born by C-section without any complication during the prenatal period. At one year of age, right bundle branch block and atrial flutter were documented (Fig. 1A, B). At 3 years, atrial flutter ablation was performed; sinus bradycardia and pauses up to 3.72 s with junctional escapes were observed after the procedure (Fig. 1C). At 5 years of age, monomorphic ventricular tachycardia (VT) was documented (Fig. 1D) and treated with lidocaine in the emergency room converting to a very slow junctional escape rhythm. A DDDR pacemaker was implanted and amiodarone treatment initiated. Two echocardiograms and a CT scan were performed ruling out structural heart disease. Clinical electrophysiological study showed a prolonged H–V interval (100 ms, normal <50 ms) and second-degree 4:3 atrioventricular (AV) conduction during atrial pacing (Fig. 1E). Radiofrequency ablation of a monomorphic VT with RBBB morphology and a cycle length of 350 ms (Fig. 1F) were attempted, without success. A pharmacological test was performed with propafenone (2 mg/kg) to unmask BrS; severe QRS widening was induced without significant changes in repolarization. The patient developed transient asystole with an acute rise in the pacing threshold, reversing spontaneously after a few seconds. The ECG was otherwise negative. The patient was clinically diagnosed as congenital

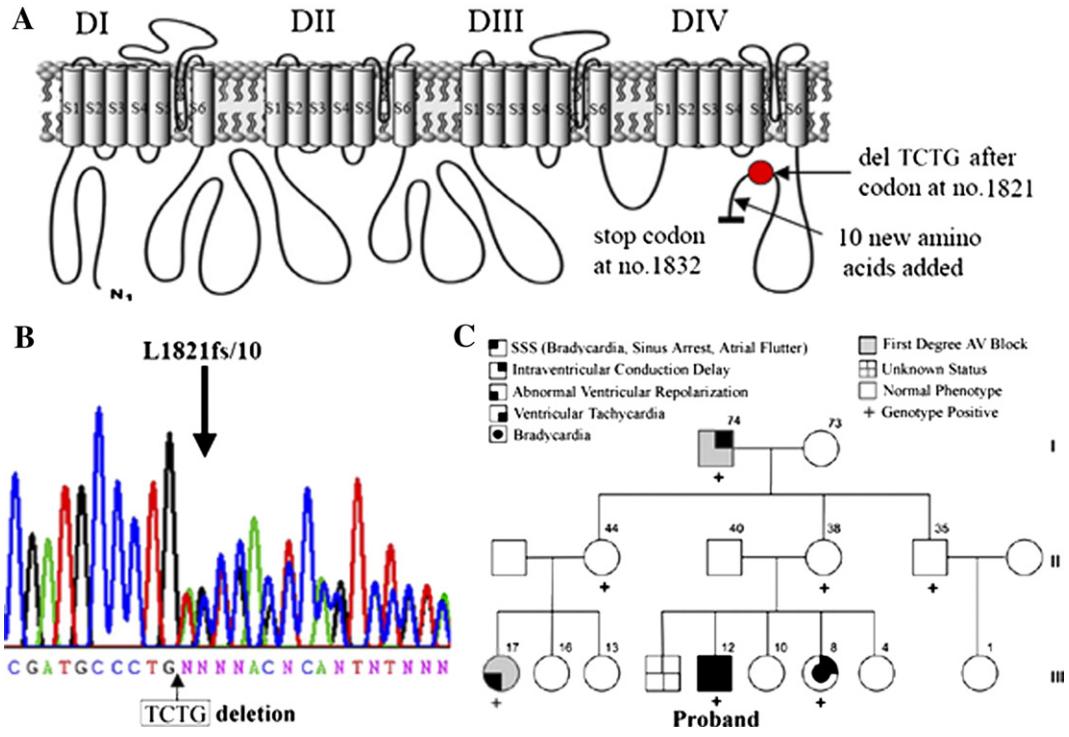

Fig. 2. (A) Topological diagram of SCN5A showing a 4 base pair deletion (TCTG) after codon at no. 1821. The deletion caused a frame shift resulting in additional 10 new amino acids added and a premature truncation of the C-terminus by a stop code (TAA) at no. 1832. (B) Sequence chromatogram for the proband. (C) Family tree showing the mutation carriers and the phenotype assignments (see symbol key). The ages of each family member is displayed above the symbol.

SSS, CCD and recurrent monomorphic VT and LQTS was also considered a possible contributor to the patient's phenotype based on QT prolongation (QTc 550 ms). However, given that torsades de pointes have never been documented, the QT prolongation might be attributed clinically to the combination of amiodarone therapy and the severity of CCD, both of which can cause QT prolongation.

3.2. Molecular characterization of L1821fs/10

A 4 base pair deletion (TCTG) at position 5464–5467 in exon 28 of *SCN5A* was elucidated (bottom panel of Fig. 2B). This deletion produced a frame-shift mutation annotated as L1821fs/10 indicating that the final normal amino acid in the protein is the leucine (L) at position 1821 followed by 10 "scrambled" (frame-shifted) amino acids before truncating prematurely. Thus, the gene product from this mutant allele ends at amino acid 1831 resulting in a severe truncation of the C-terminus.

The mutation was confirmed in the proband's mother as well (Fig. 2C) who was asymptomatic. One female sibling and one female cousin were genotype positive but had a mild clinical phenotype of bradycardia with intraventricular conduction delay and abnormal repolarization on ECG with 1st degree AV block respectively. Genotype carriers in an aunt, uncle, and grandmother were apparently asymptomatic and without ECG abnormalities. Thus, despite a severe truncation deletion predicted at the molecular/genetic level, L1821fs/10 was associated with incomplete penetrance and variable expressivity.

3.3. Expression of a C-terminal truncation mutant, L1821fs/10

Transfected HEK-293 cells transiently expressing the WT and L1821fs/10 mutant channels were voltage clamped after 24-h and 48-h incubation and showed reduced currents (Fig. 3A and B) for the mutant channel compared to WT. Summary of I_{Na} density in 3C showed that after 24 h of incubation, the mutant channel had dramatic reduction of I_{Na} density (-4 ± 2 pA/pF, $n=14$) compared to WT (-302 ± 48 pA/pF, $n=21$, p value <0.0001). Although the current density of L1821fs/10 was increased after 48 h of incubation (-22 ± 8 pA/pF, $n=33$), this was still much less than WT levels after 24 h of incubation ($p<0.001$). Note that among the 47 experiments performed for L1821fs/10, only 5 cells had macroscopic currents after 48 h of incubation sufficiently large to do kinetic analysis. Extending the incubation time to 72 h did not increase the current for L1821fs/10. Incubation with the antiarrhythmic drug (mexiletine 500 μM, quinidine 100 μM and cisapride 10 μM), and other attempts to restore the current density in L1821fs/10 such as incubation at low temperature and co-expression with the β1 and β3 subunits, known to increase I_{Na} density of some expression defect mutants, failed to restore the current densities for L1821fs/10 (data not shown). When

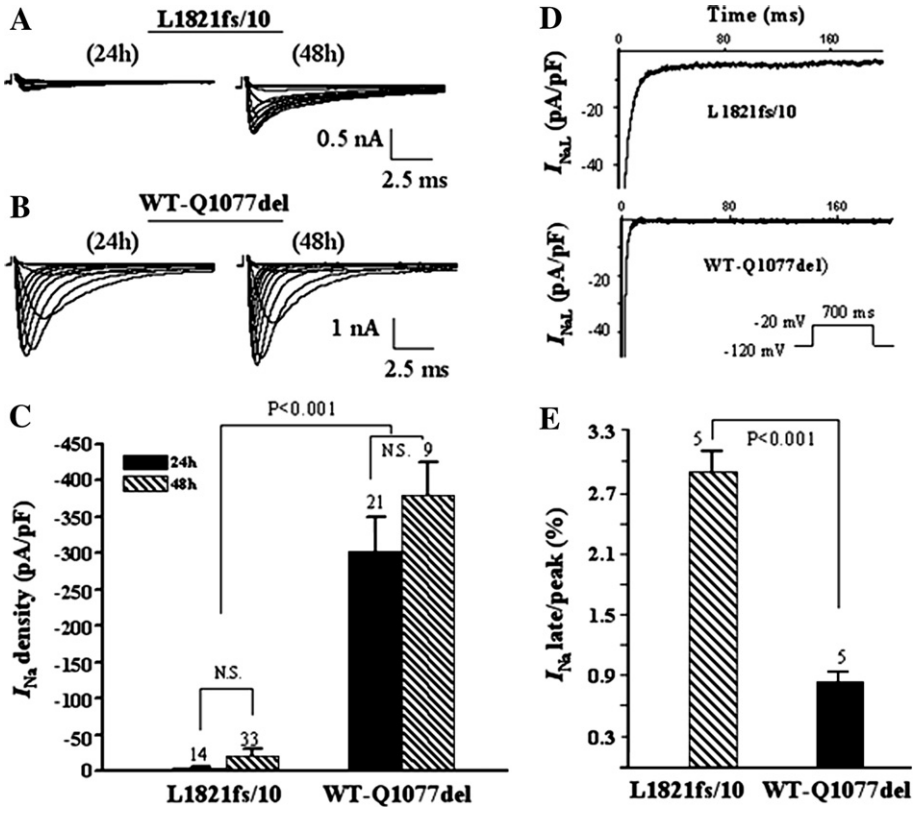

Fig. 3. Comparing the peak or late current of mutant L1821fs/10 and WT in the most common splice variant SCN5A-Q1077del background. (A, B) Whole-cell current traces from representative experiments of L1821fs/10 (A) and WT (B) after 24 h (left panel) and 48 h (right panel) transfection. (C) Summary of I_{Na} density in L1821fs/10 and WT after 24 h and 48 h of incubation. The number of experiments is indicated above the bar. N.S. indicates no significant difference. (D) Example of late I_{Na} for L1821fs/10 (top panel) and WT (bottom panel) elicited by a test depolarization pulse from −120 mV to −20 mV for 700 ms (here only 200 ms was shown). Late I_{Na} was normalized to cell capacitance, and presented in pA/pF. (E) Summary of late I_{Na} normalized to peak I_{Na}. After leak subtraction, the late I_{Na} was measured as the mean between 600 ms and 700 ms after the initiation of the depolarization. The number of experiments is indicated above the bar.

L1821fs/10 was co-expressed with WT (0.75 μg DNA each, $n=10$ cells at 24 h) the current amplitude was about 55% of that in WT alone (1.5 μg DNA $n=10$ cells) consistent with haploinsufficiency in the heterologous system, and no dominant negative effect.

Late I_{Na}, for L1821fs/10 mutant channels was increased in response to long (700 ms) depolarizing steps to various test potentials from a holding potential of −140 mV (Fig. 3D). After leak subtraction, late I_{Na} was measured as the mean between 600 and 700 ms after the initiation of the depolarization and normalized by dividing by the maximum peak amplitude of I_{Na} from the current–voltage relationship (Fig. 3E, 2.9%±0.3%, $n=5$, for L1821fs/10 and 0.8%± 0.1%, $n=5$, for WT, $p<0.001$). Late I_{Na} was confirmed using 1 μM STX (data not shown).

3.4. Voltage-dependent gating properties of L1821fs/10

Table 1 and Fig. 4 summarize voltage-dependent gating for L1821fs/10 and WT channels. The voltage-dependent activation mid-point was significantly positive shifted by 5 mV, and the slope factor was larger for L1821fs/10 compared to WT (Table 1 and Fig. 4A). The steady state inactivation mid-point was significantly negative shifted by 12 mV, and slope factor was larger for L1821fs/10 compared to WT (Table 1 and Fig. 4B). Slower time constants of recovery were observed for L1821fs/10 compared to WT (Table 1 and Fig. 4C). The mutant channel showed enhanced intermediate inactivation compared with WT for prepulse durations longer than 50 ms (Fig. 4D). The voltage dependence of decay of the current traces (Fig. 5) showed that the mutation lost the voltage dependence of decay, with the decay being slower than WT over the range of potentials >−30 mV where inactivation dominates the decay phase relative to deactivation at more negative potentials.

The voltage dependence of time to peak amplitude of I_{Na}, time constants of I_{Na} decay, and fractional amplitude of I_{Na} decay were measured at the test potentials of −50, −40, −30, −20, −10, 0, 10, 20, and 30 mV (summary data in Fig. 5). The I_{Na} for L1821fs/10 tended to peak earlier than the WT at −50 mV, but tended to peak later at more depolarized potentials (Fig. 5A). Like time to peak, the fast and slow decay time constants were faster at −50 mV for L1821fs/10 but were significantly slower for the depolarization > −20 mV compared with WT channels (Fig. 5B, C). This

Table 1
Voltage-dependent gating parameters of L1821fs/10 and WT in the Q1077del background

Samples	$V_{1/2}$ (mV)	K	$V_{1/2}$ (mV)	K	τ_f (ms)	τ_s (ms)	A_s (%)
L1821fs/10	−36.5±1.2 [a]	7±0.2 [a] (5)	−95±2.8 [a]	6±0.1 [a] (5)	2.8±0.3 [a]	57±6 [a]	18±1.5 (5)
WT	−41.5±1.5	4±0.2 (8)	−83±1.5	5±0.2 (8)	1.6±0.2	38±5	23±1.9 (10)

The fitted values of voltage-dependent gating parameters represent the mean±SEM for number of experiments in the parentheses. These parameters were obtained from fitting the individual experiments as in Fig. 4 (A, B, C) to the appropriate model equations. For the Boltzmann fits the parameters of $V_{1/2}$ are the mid-point of activation and inactivation. For the double exponential fits the parameters of recovery are: τ_f, the fast time constant; τ_s, the slow time constant; and A_s, the fractional amplitude of slow component. All parameters were analyzed by one-way ANOVA across the WT and mutant channel.
[a] Statistically significant values compared with WT.

result of slower inactivation may account for the gain of the late I_{Na} for mutated channel.

3.5. Localization of WT and L1821fs/10 mutated sodium channel proteins

Transfected or nontransfected HEK-293 cells were labeled with anti-FLAG antibody (Fig. 6A: in nonpermeabilized cells, and left panel of Fig. 6B: in permeabilized cells) to mark the location of channels. Calnexin is a chaperon protein present in the endoplasmic reticulum and was used as an endoplasmic reticulum marker with anti-calnexin antibody labeling (middle panel of Fig. 6B) to show colocalization of both markers. Forty-eight hours post-transfection, both WT and mutant had a similar peripheral SCN5A localization. Thus L1821fs/10 reached the plasma membrane ruling out a loss-of-function mechanism involving defective trafficking as the sole defect.

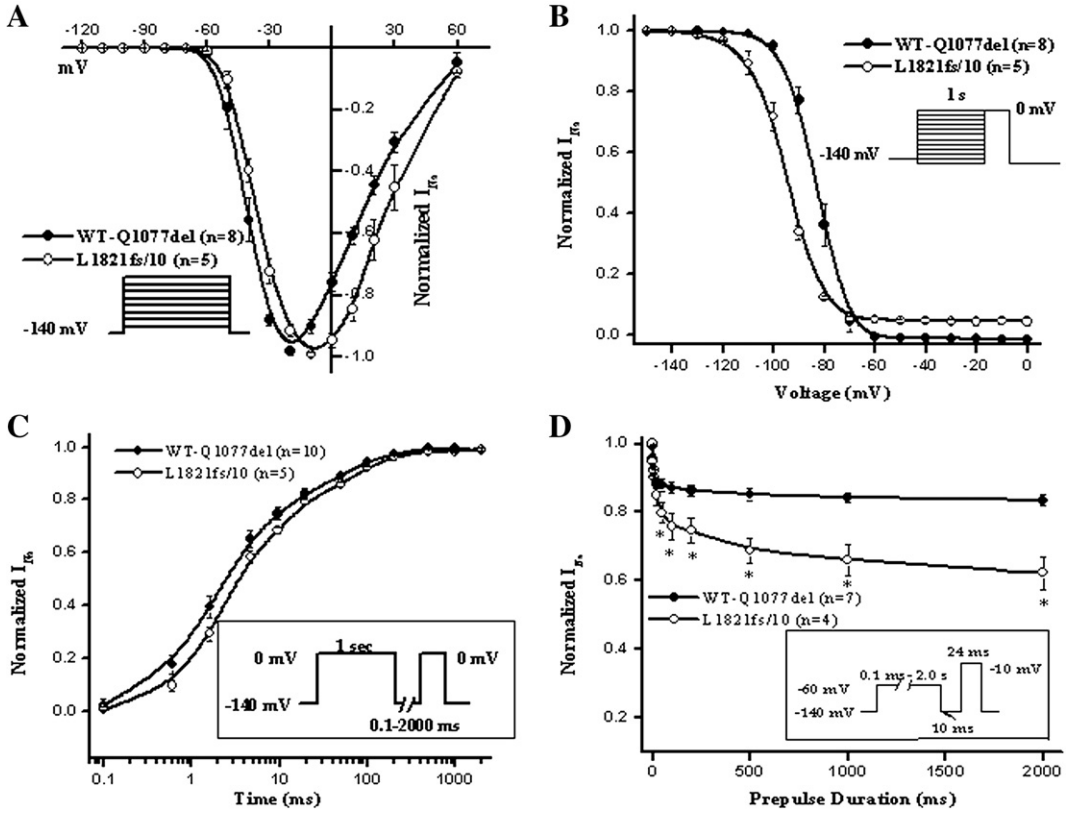

Fig. 4. Voltage-dependent gating for L1821fs/10 and WT in the Q1077del splice variant background. (A) Voltage dependence of activation for L1821fs/10 and WT. The line represents a fit to the Boltzmann function where $G_{Na}=[1+\exp(V_{1/2}-V)/\kappa]^{-1}$, where $V_{1/2}$ and κ are the mid-point and the slope factor (as an index of voltage control, all factors were more than 4), respectively, and $G_{Na}=I_{Na(norm)}/(V-V_{rev})$, where V_{rev} is the reversal potential and V is the membrane potential. (B) Steady state availability from inactivation for L1821fs/10 and WT. The line represents a fit to the Boltzmann function: $I_{Na}=I_{Na\text{-}max}[1+\exp(V_c-V_{1/2})/\kappa]^{-1}$, where the $V_{1/2}$ and κ are the mid-point and the slope factor, respectively, and V_c is the membrane potential. (C) Recovery from inactivation for L1821fs/10 and WT with time on a log scale to better show the early time course of recovery. The recovery time course was best fit with two exponentials: normalized $I_{Na}=[A_f \exp(-t/\tau_f)]+[A_s \exp(-t/\tau_s)]$ where t is the recovery time interval, τ_f and τ_s are the fast and slow time constant, and A_f and A_s are the fractional amplitude of the fast and slow recovery components respectively. (D) Intermediate inactivation for L1821fs/10 and WT channels with a variant time of the prepulse duration. All data points in this figure are shown as the mean value and the bars represent the standard error of the mean. The N numbers and fit parameters are given in Table 1. *Statistically significant differences for L1821fs/10 vs. WT.

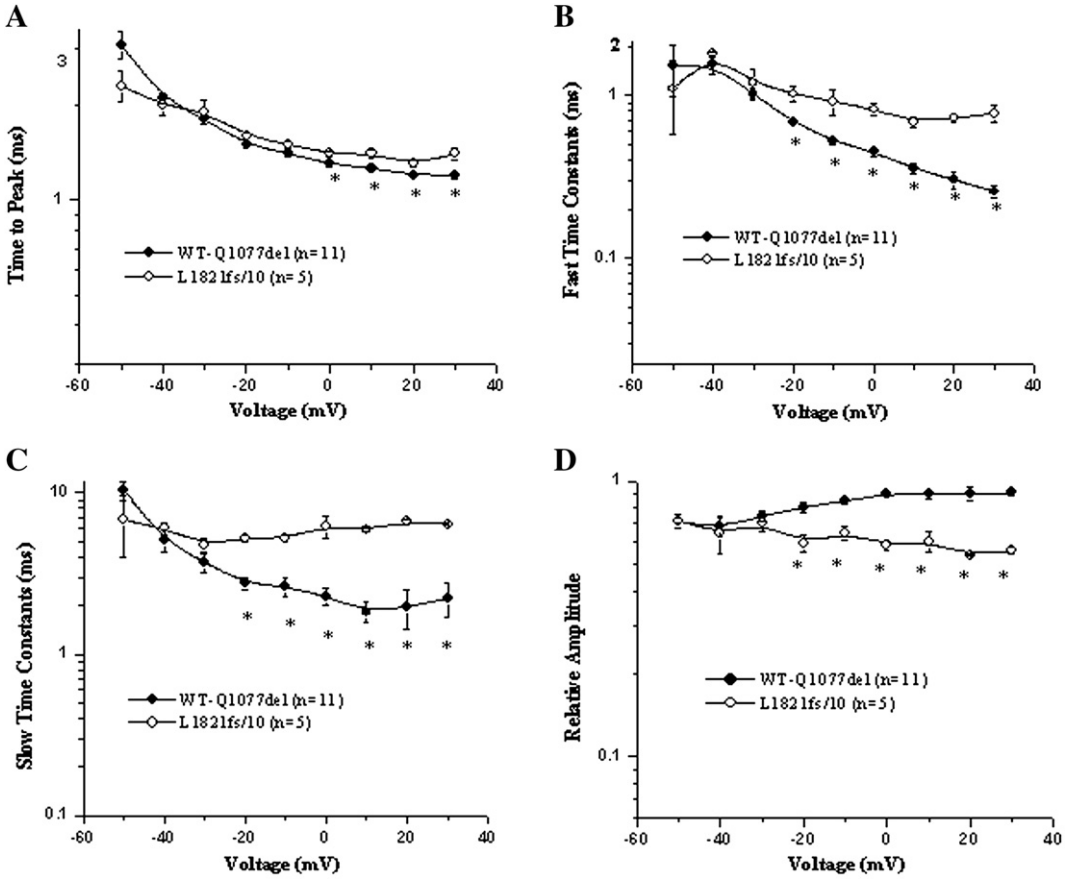

Fig. 5. Voltage dependence of time to peak (A), fast time constant (B), slow time constant (C), and fast fractional amplitude of current decay (D). Cells with comparable mean peak current amplitudes were chosen to help control for any effects that might arise from imperfect voltage control. All of the values for L1821fs/10 (opened circle) and WT (filled circle) are plotted against the test potential used to elicit I_{Na}. Time to peak is the time from the onset of depolarization to peak I_{Na}. To obtain decay rates and components, the portion of the trace from 90% of peak I_{Na} to 24 ms was fit with a sum of exponentials (exp): $I_{Na}(t) = 1 - [A_f \exp(-t/\tau_f) + A_s \exp(-t/\tau_s)] + \text{offset}$, where t is time, and A_f and A_s are fractional amplitudes of fast and slow components, respectively. Symbols represent means, and bars represent the standard error of the mean. *Statistically significant differences for L1821fs/10 vs. WT.

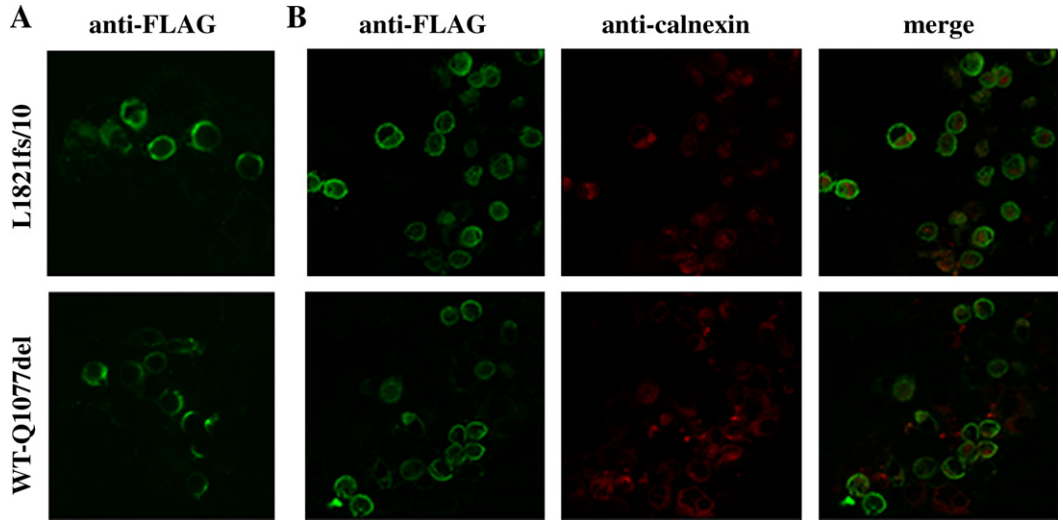

Fig. 6. Confocal images of HEK-293 cells expressing the L1821fs/10 (top panel) and WT (bottom panel) with FLAG-tagged sodium channels. (A) Surface staining of nonpermeabilized cells using anti-FLAG antibody. (B) Double staining of permeabilized cells using anti-FLAG (green) and anti-calnexin (red) antibody to show colocalization.

4. Discussion

The mutant channel L1821fs/10 exhibited a loss-of-function biophysical phenotype resulting in a mixed clinical syndrome characterized by SSS, CCD and recurrent VT. This discovery provides the fifth *SCN5A* mutation associated with multiple clinical phenotypes [7–10]. Generally, mutations in *SCN5A* that cause a decrease in peak I_{Na} density appear to be associated with BrS1/CCD [3,5,9]. This can occur by two general mechanisms: a decrease in channel expression or a change in channel kinetics that tends to decrease peak I_{Na}.

How does a loss-of-function mutation in some patients cause BrS1, SSS, or CCD, or in some patients, mixtures of these syndromes? It has been proposed [18] that a rightward shift in the voltage dependence of the mutant sodium channel activation curve, as found with L1821fs/10 (Fig. 4A) is a common feature of CCD [5,9,10,19]. The slower time to peak I_{Na} (Fig. 5A) in our study indicates that the mutant channels require a more positive membrane potential to fully activate and more time to reach the membrane potential at which the maximum current amplitude occurs than WT channels, which might manifest on the ECG in a widening of the QRS in CCD [5,10,18,19]. However, the mechanisms by which the proband showed SSS and monomorphic VT but not BrS1, are unknown.

The mutation, L1821fs/10, also showed decreased I_{Na} with slow decay and a noninactivating component (late I_{Na}) in those cells that had measurable macroscopic currents (Figs. 3 and 5), similar to the gain-of-functional molecular phenotype of LQT3. This introduces seemingly paradoxical terminology, how can a mutation cause both "loss of function" and "gain of function". The key distinction is timing, "loss of function" generally refers to a loss of peak or early I_{Na}, and "gain of function" generally refers to late I_{Na}. For L1821fs/10 mutant channels, peak I_{Na} is decreased but late I_{Na} is increased relative to peak I_{Na}.

This combination of molecular phenotypes has been reported previously for ΔK1500, a deletion of a lysine in the III–IV linker of SCN5A, which is associated with BrS1, LQT3 and CCD [10] and for 1795insD, an insertion of aspartic acid in the C-terminal domain of SCN5A, which causes both LQT3 and BrS1 [8]. In heterologous expression system, L1821/fs10 also has very similar molecular phenotype of both loss-of-function and gain-of-functional sodium channel features with a previously reported mutation of a methionine to a leucine (M1766L) from a patient with LQT3 [20]. When expressed, M1766L showed a profound trafficking defect, but had increased late I_{Na} and the expression defect was "rescued" by mexiletine, or, as in the patient, the mutation was rescued when expressed in the context of a sodium channel containing the common polymorphism H558R [14].

In this case, the L1821fs/10 proband did have a prolonged QTc, but it was in the presence of right bundle branch block, and his VT was monomorphic, not torsades. Although this mutation has a biophysical phenotype that could potentially cause LQT3, there is no evidence for LQT3 in the patient. The reduced current expression was not restored with mexiletine, quinidine, or cisapride, drugs previously reported to rescue expression defective SCN5A mutations [17,20–22]. Co-expression with β subunits and low temperature of incubation, which increased some expression levels in M1766L [20], did not increase expression level for L1821fs/10. Further, the cell surface staining with anti-FLAG antibody (Fig. 6A: in nonpermeabilized cells) and co-labeling with anti-Flag antibody and anti-calnexin antibody (Fig. 6B: in permeabilized cells) indicated that the L1821fs/10 channel reached the plasma membrane. From this we conclude that the markedly decreased peak I_{Na} of L1821fs/10 was mainly caused by biophysical abnormalities.

Recently, the $Na_v1.5$ C-terminal domain has attracted considerable attention for having a direct structural role in the control of channel inactivation in the studies by Kass and colleagues [11,23–25]. They postulate that the proximal part of the C-terminal domain is a critical structure for stabilizing the inactivated state of the channel during prolonged depolarization. The naturally occurring C-terminal truncation mutation, L1821/fs10 (Q1832 stop) in our study not only showed results similar to the experimental mutation (S1885 stop) designed to test biophysical function of the C-terminus, namely increased late I_{Na} resulting from channels failing to inactivate during prolonged depolarization and slows the channel's recovery from inactivation, as well as shifts the steady state inactivation curve in the hyperpolarizing direction [23–25].

It is interesting that selected family members preferentially presented the phenotype with different degrees of severity, the marked clinical phenotype suffered by the proband contrasts sharply with the lack of symptoms in four carriers in the preceding generations and the very mild clinical phenotypes observed in a sister and a cousin. In general, but with one exception, the asymptomatic carriers were females, which agrees with a male predominance for loss-of-function SCN5A mutations causing BrS1. The mechanisms for this variability in this instance and in general are incompletely understood. We previously reported that the two common polymorphisms (H558R and S524Y) caused a profound expression defect in the Q1077 background, but not the Q1077del background [16,26], and that H558R can modify expression of an arrhythmia causing mutation M1766L [14]. These and other polymorphisms were absent in these patients. Loss-of-function for the BrS1 mutation G1406R was more severe in the Q1077 background [17]. Although mRNA for Q1077 and Q1077del is present in equal ratios in different individuals [26], should the protein levels vary this could account for clinical variability. Other unknown genetic, developmental, or acquired abnormalities may also account for clinical variability. For example structural abnormalities such as increased fibrosis have been shown to interact with decreased I_{Na} [27] to affect excitability and conduction.

Understanding the mechanisms for variability of the clinical phenotype may lead to improved understanding of pathogenesis and of possible therapy.

It is important to emphasize that these studies in heterologous systems, like previous work in the field, may not reflect what occurs in the myocytes, which have additional subunits and interacting proteins. Also these clones do not contain the introns or promoters that might affect expression in the myocytes. These experiments in heterologous systems only suggest a possible biophysical phenotype that may lead to the clinical syndromes, but further studies in more integrated systems are necessary to describe the full pathogenetic pathway.

Acknowledgments

This work was supported by an American Heart Association (AHA), Greater Midwest Affiliate Postdoctoral Fellowship to BH.T., AHA Established Investigator Award to M.J.A., and NIH grant HD42569 to M.J.A and HL71092 to J.C.M.. We are particularly indebted to family members for their participation in this study.

References

[1] Goldin AL. Evolution of voltage-gated Na^+ channels. J Exp Biol 2002;205:575–84.
[2] Wang Q, Shen J, Splawski I, Atkinson D, Li Z, Robinson JL, et al. *SCN5A* mutations associated with an inherited cardiac arrhythmia, long QT syndrome. Cell 1995;80:805–11.
[3] Chen Q, Kirsch GE, Zhang D, Brugada R, Brugada J, Brugada P, et al. Genetic basis and molecular mechanism for idiopathic ventricular fibrillation. Nature 1998;392:293–6.
[4] Schott JJ, Alshinawi C, Kyndt F, Probst V, Hoorntje TM, Hulsbeek M, et al. Cardiac conduction defects associate with mutations in SCN5A. Nat Genet 1999;23:20–1.
[5] Tan HL, Bink-Boelkens MTE, Bezzina CR, Viswanathan PC, Beaufort-Krol GC, van Tintelen PJ, et al. A sodium-channel mutation causes isolated cardiac conduction disease. Nature 2001;409:1043–7.
[6] Benson DW, Wang DW, Dyment M, Knilans TK, Fish FA, Strieper MJ, et al. Congenital sick sinus syndrome caused by recessive mutations in the cardiac sodium channel gene (*SCN5A*). J Clin Invest 2003;112:1019–28.
[7] Smits JPP, Koopmann TT, Wilders R, Veldkamp MW, Opthof T, Bhuiyan ZA, et al. A mutation in the human cardiac sodium channel (E161K) contributes to sick sinus syndrome, conduction disease and Brugada syndrome in two families. JMCC 2005;38:969–81.
[8] Bezzina C, Veldkamp MW, van den Berg MP, Postma AV, Rook MB, Viersma JW, et al. A single Na+ channel mutation causing both long-QT and Brugada syndromes. Circ Res 1999;85:1206–13.
[9] Kyndt F, Probst V, Potet F, Demolombe S, Chevallier JC, Baro I, Moisan JP, et al. Novel *SCN5A* mutation leading either to isolated cardiac conduction defect or Brugada syndrome in a large French family. Circulation 2001;104:3081–6.
[10] Grant AO, Carboni MP, Neplioueva V, Starmer CF, Memmi M, Napolitano C, et al. Long QT syndrome, Brugada syndrome, and conduction system disease are linked to a single sodium channel mutation. J Clin Invest 2002;110:1201–9.
[11] Glaaser IW, Bankston JR, Liu H, Tateyama M, Kass RS. A carboxy terminal hydrophobic interface is cortical to sodium channel function: relevance to inherited disorders. J Biol Chem 2006;281(33):24015–23.
[12] Ackerman MJ, Siu BL, Sturner WQ, Tester DJ, Valdivia CR, Makielski JC, et al. Postmortem molecular analysis of SCN5A defects in sudden infant death syndrome. JAMA 2001;286(18):2264–9.
[13] Van Driest SL, Ackerman MJ, Ommen SR, Shakur R, Will ML, Nishimura RA, et al. Prevalence and severity of "benign" mutations in the beta-myosin heavy chain, cardiac troponin T, and alpha-tropomyosin genes in hypertrophic cardiomyopathy. Circulation 2002;106(24):3085–90.
[14] Ye B, Valdivia CR, Ackerman MJ, Makielski JC. A common human SCN5A polymorphism modifies expression of an arrhythmia causing mutation. Physiol Genomics 2003;12:187–93.
[15] Nagatomo T, Fan Z, Ye B, Tonkovich GS, January CT, Kyle JW, et al. Temperature dependence of early and late currents in human cardiac wild-type and long QT Δ KPQ Na^+ channels. Am J Physiol 1998;275:H2016–24 (Heart 44).
[16] Tan BH, Valdivia CR, Rok BA, Ye B, Ruwaldt KM, Tester DJ, et al. Common human SCN5A polymorphisms have altered electrophysiology when expressed in Q1077 splice variants. Heart Rhythm 2005;2:741–7.
[17] Tan BH, Valdivia CR, Song C, Makielski JC. Partial expression defect for the *SCN5A* missense mutation G1406R depends upon splice variant background Q1077 and rescue by mexiletine. Am J Physiol Heart Circ Physiol 2006;291(4):H1822–8.
[18] Clancy CE, Kass RS. Defective cardiac ion channels: from mutations to clinical syndromes. J Clin Invest 2002;110:1075–7.
[19] Shirai N, Makita N, Sassaki K, Yokoi H, Sakuma I, Sakurada H, et al. A mutant cardiac sodium channel with multiple biophysical defects associated with overlapping clinical features of Brugada syndrome and cardiac conduction disease. Cardiovasc Res 2002;53:348–54.
[20] Valdivia CR, Ackerman MJ, Tester DA, Wada T, McCormack J, Ye B, et al. A novel *SCN5A* arrhythmia mutation, M1766L, with expression defect rescued by mexiletine. Cardiovasc Res 2002;54:624–9.
[21] Liu K, Yang T, Viswanathan PC, Roden DM. New mechanism contributing to drug-induced arrhythmia: rescue of a misprocessed LQT3 mutant. Circulation 2005;112:3239–46.
[22] Valdivia CR, Tester DJ, Rok BA, Porter CB, Munger TM, Jahangir A, et al. A trafficking defective, Brugada syndrome-causing SCN5A mutation rescued by drugs. Cardiovasc Res 2004;62:53–62.
[23] Cormier JW, Rivolta I, Tateyama M, Yang AS, Kass RS. Secondary structure of the human cardiac Na^+ channel C terminus. J Biol Chem 2002;277:9233–41.
[24] Motoike HK, Liu H, Glaaser IW, Yang AS, Tateyama M, Kass RS. The Na^+ channel inactivation gate is molecular complex: a novel role of the COOH-terminal domain. J Gen Physiol 2004;123:155–65.
[25] Kass RS. Sodium channel inactivation in heart: a novel role of the carboxy-terminal domain. J Cardiovasc Electrophysiol 2006;17:S21–5.
[26] Makielski JC, Ye B, Valdivia CR, Pagel MD, Pu JL, Tester DJ, et al. A ubiquitous splice variant and a common polymorphism affect heterologous expression of recombinant human SCN5A heart sodium channels. Circ Res 2003;93:821–8.
[27] Van Veen TA, Stein M, Royer A, Le Quang K, Charpentier F, Colledge WH, et al. Impaired impulse propagation in *Scn5a*-knockout mice. Combined contribution of excitability, connexin expression, and tissue architecture in relation to aging. Circulation 2005;112:1927–35.